NASA

Technical Memorandum 86052

Voyager Observations of Jovian Millisecond Radio Bursts

Joseph K. Alexander and Michael D. Desch

JANUARY 1984

National Aeronautics and Space Administration

Goddard Space Flight Center
Greenbelt, Maryland 20771

VOYAGER OBSERVATIONS OF JOVIAN MILLISECOND RADIO BURSTS

J. K. Alexander and M. D. Desch

NASA/Goddard Space Flight Center
Laboratory for Extraterrestrial Physics
Planetary Magnetospheres Branch
Greenbelt, Maryland 20771

Abstract

Voyager Planetary Radio Astronomy data collected over 30-day intervals centered on the two close encounters with Jupiter have been utilized to study the characteristics of millisecond-duration radio bursts (s-bursts) at frequencies between 5 and 15 MHz. In this frequency range, s-bursts are found to occur almost independently of Central Meridian Longitude and to depend entirely on the phase of Io with respect to the observer's planetocentric line of sight. Individual bursts typically cover a total frequency range of about 1.5 to 3 MHz, and they are usually strongly circularly polarized. Most bursts in a particular s-burst storm will exhibit the same polarization sense (either right-hand or left-hand), and there is some evidence for a systematic pattern in which one polarization sense is preferred over the other as a function of Io phase and Central Meridian Longitude. These data are all suggestive of a radio source that is located along the instantaneous Io flux tube and that extends over a linear dimension of $\sim$ 5000 km along the field lines in both the northern and southern hemispheres.

Introduction

Jupiter's decameter-wavelength radio emisions exhibit temporal variations on at least three distinct time scales that are short compared to the planet's 10-hr rotation period. The most common of these appears as a pronounced variation in intensity over an interval of a few minutes at any given wave frequency and is now known to correspond to the remarkable curved features ('dynamic-spectral arcs') seen in plots of intensity as a function of frequency and time (e.g., see Boischot et al. [1981] or Carr et al. [1983]). The next shorter time-scale variation can be seen in high resolution dynamic spectra as a series of narrow lanes ('modulation lanes') that drift in frequency at $\sim$ ±100 kHz/sec. Modulation lanes have durations of $\sim$ 1 sec at a given frequency and occur quasi-periodically at intervals of several seconds (e.g., Riihimaa [1970] or Genova et al. [1981]). Finally, at the shortest time scale there exist intense short bursts ('s-bursts') that have characteristic durations of several milliseconds and that drift rapidly in frequency at about -10 MHz/sec or faster. Observations of Jupiter's decametric emission obtained from ground-based radio telescopes show

additional classes of temporal structure on scales of ∿ 1 sec and ∿ 1 min, but they are due to propagation effects imposed on the Jovian signals by the interplanetary medium and the terrestrial ionosphere, respectively, rather than by processes in the Jovian environment. Of the former three types of temporal variations, only the fast s-bursts have been established convincingly as originating from an intrinsic aspect of the emission mechanism itself.

In this paper we present new measurements of the properties of s-bursts obtained with the Voyager-1 and 2 Planetary Radio Astronomy instruments when the spacecraft were near their close approaches to Jupiter in 1979. Although when operating in their normal survey mode the Voyager receivers cannot resolve individual s-bursts, Leblanc and Genova [1981] have shown that s-burst episodes are often easily recognized in the dynamic spectral plots. Consequently, measurements of some gross properties of the s-bursts and certain kinds of statistical studies are feasible without requiring millisecond time resolution. Leblanc and Genova [1981] concentrated on events at frequencies above 15 MHz and showed that the high frequency s-bursts detected both before and after the Voyager-Jupiter encounters fell into two tightly confined regions when diagrammed as a function of Central Meridian Longitude (CML) and angular departure of Io from superior conjunction with the observer's line of sight (ϕIo). These two regions, which Leblanc denoted S-IoB and S-IoA'C, are coincident with the regions in the ϕIo-CML plane in which s-bursts are observed between 15 and 40 MHz with ground-based radio telescopes [Leblanc et al., 1980]. We will extend the earlier survey of Voyager data to lower frequencies, concentrating on the range 5-15 MHz where ϕIo-CML occurrence patterns imply strong Io dependence but no dependence on CML. We will also present new evidence concerning the bandwidth over which groups of s-bursts may occur and will relate that frequency range to the spatial scale of the source. Finally, we will examine the polarization of s-bursts at frequencies near 10 MHz. In many ways this study is complementary to an analysis by Ellis [1982] who studied the properties of s-bursts between 3.2 and 32 MHz using ground-based observations collected between 1972 and 1980.

Observations

The Voyager Planetary Radio Astronomy receivers cover a frequency range

from 1.2 kHz to 40.5 MHz. They are usually operated in a frequency scanning mode in which the entire frequency range is scanned once every 6 sec by sampling 198 separate frequency steps with a dwell time of 30 ms on each step (25 ms integration time after 5 ms for local oscillator settling). In the spectral range of interest in this study ($\geq$ 1.3 MHz) each frequency channel has a bandwidth of 200 kHz, and the separation between steps is 307 kHz. Thus, a given 25 ms x 200 kHz data sample could envelop a number of s-bursts. (See Lang and Peltzer [1977] for a more detailed description of the receiver design.)

The detection of s-bursts in this receiver mode is illustrated schematically in Figure 1. A sequence of five consecutive data samples is plotted as a function of frequency and time. Each sample is integrated over a 200 kHz bandwidth for 25 ms and the center frequency is changed by 307 kHz every 30 ms. The labels "RH" and "LH" inside each sample denote the fact that individual measurements alternate in being sensitive to either right-hand or left-hand circularly polarized signals. The drift rate measured for s-bursts in the 10-15 MHz frequency range is typically -10 MHz/sec [Ellis, 1980], and Ellis' atlas of burst dynamic spectra [1979] shows them occurring at intervals ranging from about 20 ms to more than 100 ms in this frequency range. Thus, the slanted lines represent a group of s-bursts drifting across a 500-kHz band in the frequency range being sampled. The darkened line segments denote the portions of the s-bursts that would be detected by the Voyager receiver. They would show up as intensity enhancements in two or three adjacent frequency channels, and if the s-burst emission persisted for less than a few seconds no emission would be detected during the next scan 6 sec later. Because the Voyager receivers' frequency stepping rate is also 10 MHz/sec, it is optimally suited for following s-bursts as they drift through the 15 to 5 MHz band. Moreover, variations in impedance of the 10-m antenna monopoles employed on Voyager lead to the best impedance match to the receivers at $\sim$ 10 MHz (T. D. Carr, private communication) so that the highest sensitivity to decametric signals also occurs in this range. The Voyager instruments' wide frequency coverage and ability to monitor Jupiter continuously with high sensitivity thereby provide a unique set of measurements of the occurrence statistics, total bandwidth and polarization of low frequency s-bursts.

Examples of s-bursts in the decametric dynamic spectra are shown in Figure 2. Here each panel is a plot of signal intensity (indicated by darkness of the grey shading) measured between 1.3 and 40.5 MHz over a 60-min time interval. Individual frequency scans are repeated every 6 sec. The values of CML and ϕIo as seen from the spacecraft at the beginning of each plot are indicated in the lower left-hand corner of each panel. The examples shown in the top and middle panels (taken from Voyager-2) correspond to Io-B events, and the example in the bottom panel in Figure 2 (taken from Voyager-1) corresponds to an Io-C event. The s-bursts can be recognized as dark (i.e., intense), short, vertical streaks that appear several times per minute between about 8 and 15 MHz. They are particularly visible between about 1240 and 1250 on July 12, 1979 (upper panel), between about 2230 and 2240 on July 17, 1979 (middle panel), and between 0250 and 0300 on March 6, 1979 (bottom panel). Notice that the frequency range covered by s-bursts captured during a particular 6-sec frequency scan can be estimated by the length along the frequency axis of the individual streaks.

In the first 30-min of the lower panel in Figure 2 (March 6, 1979) one can see two narrow bands of emission that drift slowly downward in frequency from about 26 and 20 MHz at 0220 to 20 and 16 MHz at 0250. The lower frequency member of this pair, and also the similar band in the right-hand side of the upper panel, are probably the same as the narrow-band emissions described by Riihimaa (1977) and by Leblanc and Rubio [1982] and called "n-events" by Carr et al. (1983). These bands may actually be a train of unresolved s-bursts, but since that identification cannot be made unambiguously with the Voyager data, we have not included such events in our s-burst data set.

The results in this paper are based on a survey of s-burst episodes seen in spectrograms like those shown in Figure 2 covering 30-day intervals centered on the encounters with Jupiter by Voyager-1 on March 5, 1979 and Voyager-2 on July 9, 1979. S-bursts were identified by their impulsive character which is usually easily distinguished from the decametric arcs that vary in intensity in a minute or more rather than in 6 sec. Groups of s-bursts that persist for less than 6-sec in a given frequency band may be favored slightly in the survey (compared to longer burst trains) because

enhancements that occur on one scan but not on the adjacent scans 6 sec earlier or later are more easily recognized as s-bursts than would be continuous burst emission at the same frequency for several consecutive scans. There is also a bias in our survey against the detection of events that cover a frequency band of less than 300 kHz, because events that contribute to only a single plot pixel (i.e., one data sample in a scan) were not considered to be sufficiently reliable to be catalogued. Likewise, bursts that drift substantially slower than -10 MHz/sec would not contribute to more than one plot pixel, and so they also will not be included in our survey.

Occurrence Statistics

The present study is based on approximately 1400 hours of observations from the two Voyager encounter periods. We have identified a total of about 54 hours of s-burst activity over this interval corresponding to an average probability of occurrence of s-burst episodes of about 4%. As we shall see later, the low occurrence probability of s-burst storms is due, in part, to the very narrow range of geometrical locations of Io during which s-bursts can be observed. The two spacecraft approached Jupiter from above the pre-noon Jovian local time (L.T.) sector at small positive Jovigraphic latitudes (1100 L.T. and $+3^\circ$ latitude for Voyager-1, 0930 L.T. and $+7^\circ$ latitude for Voyager-2), and they receded from the planet in the pre-dawn sector (0400 L.T. for Voyager-1 and 0300 L.T. for Voyager-2) at $+5^\circ$ Jovigraphic latitude after encounter. When we compare the s-burst occurrence probabilities and occurrence patterns as a function of CML and ϕIo, we find no significant differences in the results either between the data collected by the two spacecraft or between the pre-encounter and post-encounter legs of the spacecraft trajectories. Thus, within the statistical limitations of the data set used in the study, there is no evidence for either a strong latitudinal dependence or a local time dependence in the s-bursts at low frequencies. They appear distinct in this respect from some components of the smoother dynamic spectral arc emissions which do exhibit certain dependences on local time and latitude (see Carr et al. [1983]).

The occurrence of s-bursts detected from Voyager is shown as a function of CML and ϕIo in Figure 3. At frequencies above 15 MHz (top panel of Figure

3) the s-burst events are confined to a very specific range of values of both CML and ϕIo. These are the S-IoB and S-IoA'C regions already described by Leblanc and Genova [1981] on the basis of ground-based and Voyager observations at frequencies above 15 MHz. At lower frequencies in the 5 to 15 MHz range (middle panel of Figure 3) we find that the s-bursts no longer depend on CML, but they can occur instead at any longitude. The dependence on ϕIo, on the other hand, remains very strong. Thus, the Voyager measurements corroberate the findings of Witham [1978] and Ellis [1982] who used a smaller set of ground-based observations between 8 and 24 MHz and concluded that below 17 MHz s-bursts depended only on the position of Io. A minor exception to the property of CML-independence at low frequencies is the tendency for the band of activity at ϕIo $\sim$ 230° to show a gap for 150° < CML < 240° (Figure 3b). This pattern is also evident in the data presented by Ellis [1982].

One-dimensional Io phase histograms of s-burst activity above and below 15 MHz are shown in the bottom panel in Figure 3. Here we clearly see the effect noted earlier by Riihimaa [1977] and others whereby the s-bursts tend to occur at slightly lower values of ϕIo than do the smoother emissions that comprise the dynamic spectral arcs. In the 15-25 MHz range the s-bursts have a ϕIo peak at 80°-85°, and they cut off abruptly at ϕIo = 90°. The Io-related arc emissions, on the other hand, show an occurrence maximum at ϕIo = 90° (e.g., see Carr et al. [1983], and references therein). The 5-15 MHz s-bursts also peak below ϕIo = 90°, but they are found to occur in a band that extends as far above 90° as it does below. The second peak in the ϕIo histogram falls at about 230° for s-bursts between 5 and 15 MHz and at 220°-225° for the 15-25 MHz frequency range in contrast to the Io-related A and C arc emissions which are centered at ϕIo = 240°.

The apparently anomalous activity that appears in Figure 3c near ϕIo = 180° and 340° is due in both cases to s-bursts observed near the time of closest approach to Jupiter. In particular, the 180° emissions were observed by Voyager 1 on March 5, 1979 from a range of less than 6 R_J. The s-bursts at about 340° ϕIo were observed from Voyager-2 on July 9, 1979 just inside a Jovicentric distance of 13 R_J.

Finally, we can see from Figure 3 that there were nearly twice as many

s-burst events detected near ϕIo $\sim$ 90° as there were in the band near ϕIo = 230°. Riihimaa [1977] obtained essentially the same result between 21 and 30 MHz in his ground-based surveys between 1963 and 1976. One reason for this difference is the enhanced occurrence rate in the region of the Io-B geometry where 110° < CML < 210°. Another reason for this effect is the relative sparsity of activity near 230° ϕIo when 150° < CML < 240°. Given the high sensitivity of the Voyager measurements near Jupiter, we conclude that the greater likelihood of s-burst activity when ϕIo is near 90° is not simply a manifestation of systematically higher burst intensities for that geometry. In view of the fact that there are more ϕIo $\sim$ 90° than ϕIo $\sim$ 230° events when viewing Jupiter both from above the sunlit hemisphere (before closest approach) and from above the night hemisphere (after closest approach), we can also conclude that this effect does not reflect some diurnal asymmetry of the sort that occurs in the Io-independent decametric emissions [Alexander et al., 1981]. Instead, the greater proclivity for s-burst emissions to be detected when Io is at early phase angles with respect to the observer may reflect a tendency for the radio waves to escape more readily toward the direction of lower System III longitudes relative to the location of the radio source than in the opposite direction (i.e., toward higher longitudes).

Burst Frequency Extent

One property of individual s-bursts that can be estimated from the Voyager data is the maximum frequency excursion of a burst (or burst group) over which the burst(s) can be tracked. The ground-based observations between 3 and 32 MHz reported by Ellis [1982] yielded values for the frequency range of individual s-bursts between 0.5 and 1.8 MHz. At 10 MHz, Ellis found the burst frequency range to have an average value of about 1 MHz, and this is also the case for the Voyager data between 5 and 15 MHz. Because the apparent frequency range of an s-burst detected by the Voyager instruments may be determined in part by the frequency range over which the burst drift rate and receiver sweep rate are comparable, we believe the most meaningful Voyager measurements are of the maximum frequency excursion over which individual bursts can be seen in an episode.

We have estimated the maximum frequency range covered by individual

s-bursts in each of the 84 s-burst episodes (or storms) in our survey, and a histogram of the distribution of maximum burst frequency extent is shown in Figure 4. We find that both the modal and mean values for the maximum burst frequency range are near 1.8 MHz (std. dev. = 0.9 MHz). This is in agreement with Ellis [1982] who showed a maximum value of about 1.4 to 1.5 MHz for bursts observed near 10 MHz. One can also see from Figure 4 that there are a few cases in which individual s-bursts appear to extend over at least 3 MHz and possibly as much as 5 MHz. A detailed, case-by-case examination of some of these events suggests that the 5 MHz bursts may actually correspond to the superposition of several more narrow bursts at slightly different frequencies. There are a number of clear examples of 3 MHz events, however, that appear to reflect the true frequency extent of a single burst.

If one adopts the commonly accepted model of s-bursts as being generated by bunches of nearly monoenergetic electrons that are ascending magnetic field lines and exciting radiation near the local electron gyrofrequency [Desch et al., 1978], then the maximum frequency range over which s-bursts can be tracked gives an estimate of the minimum distance along the field line over which the electrons must maintain coherence in some way that leads to the intense s-burst radiation. For the bursts observed near 10 MHz the average value of the maximum frequency range of 1.8 MHz (Figure 5) corresponds to a minimum distance along a field line in the O_4 magnetic field model [Acuna and Ness, 1976] of about 3800 km. The extreme value of 3 MHz observed for $120° < CML < 200°$ corresponds to lengths along a field line of about 6500 km.

If the s-burst emission is beamed into a radiation pattern that takes the form of a thin sheet, then the total observed frequency range will also be limited by the angular thickness of the sheet and the range of points along the field line from which one can detect the radiation before field line curvature tilts the beam out of the line of sight. Ellis [1982] used this concept to try to estimate the angular thickness of the s-burst radiation pattern. His results may not be valid below 15 MHz however, because he considered the effect of field line curvature in a meridian plane. The problem with Ellis' calculation becomes clear when we note that the strong Io phase dependence of low-frequency s-bursts evident in Figure 3 suggests that the meridian planes containing the source field lines probably lie at

significant angular distances away from the observer's line of sight (i.e., nearer $\phi Io \sim 80°$ and $230°$ than $\phi Io \sim 180°$). Therefore the field line curvature out of the meridian plane of the source is likely to be equally important in limiting the visible frequency range as is the curvature in the meridian plane. This complication makes an estimate of the angular properties of the radiation more difficult, and it reinforces the point that the estimates of path length along the field line for "beam coherence" are truly lower limits.

S-burst Polarization

The Voyager PRA receiver determines emission polarization sense by sampling the circularly polarized power (left hand or right hand) at one frequency, followed 30 millisec later by the reverse polarization at the adjacent frequency and so on, until all 198 channels have been sampled. On the succeeding frequency sweep, the polarization sense measured at any given frequency is reversed. Thus, although simultaneous polarization measurements are not made, the polarization sense can be determined if the total emission bandwidth extends over a sufficiently broad frequency range or if it endures longer than a few (6-sec) sweeps. In the case of the s-bursts, an unambiguous polarization sense determination can be made provided the burst appears on at least 4 adjacent channels, that is if it has a bandwidth of at least 1000 kHz. (A three-channel determination is possible provided the intensities of the first and third channels exceed that of the middle channel.) For the present study, this minimum bandwidth effectively constrains the observations to bursts occurring in the range 8 to 13 MHz, where the receiver sensitivity is greatest. Since the PRA receiver measures only the right-hand (RH) and left-hand (LH) circularly polarized powers, no complete determination of polarization degree, axial ratio, or wave tilt angle is possible. Abrupt polarization reversals of an instrumental origin occur near 5 and 15 MHz (see Alexander et al. [1981]), and bursts detected near those frequencies have not been used in the polarization analysis.

The polarization senses of 93 s-bursts associated with 10 separate storms have been determined. About 90% of the bursts analyzed were observed to be strongly polarized, having at least a factor of two power difference between left and right channels across the burst bandwidth. There was no tendency for

the sample as a whole to show a significant preference for one polarization sense over the other. However, most of the storms showed a strong preference to be polarized in only one sense. In fact it was usually the case that all of the bursts within a given storm were of a single polarization.

These measurements are summarized in Figure 5 where we show the polarization sense of the s-burst storms as a function of CML and Io phase. White (black) bars denote RH (LH) polarization, and the two periods of s-burst activity in which bursts of both polarizations were observed are denoted with striped bars. There appears to be a tendency for early longitude storms near 230° Io phase to be LH polarized and for late longitude storms to be RH polarized. This pattern is reversed for the storms associated with Io phase near 90°. However, the observations of s-bursts polarization in Figure 5 remain sparse. In addition, as noted, two of the storms exhibit s-bursts of both polarizations, which is not consistent with a simple polarization pattern in CML-Io phase space. It is clear, therefore, that additional measurements should be made before any generalizations with regard to polarization patterns can be made.

Of the 10 storms analyzed, one (28 s-bursts) is of special interest because of its unusual duration and CML-Io phase geometry. This storm occurred on 12 July, 1979, between 1240 and 1730 SCET (see Figure 2). The s-bursts waxed and waned in intensity, but never disappeared for more than 5 or 10 minutes at a time during the entire 290 minute interval. During this time, the CML increased from 160° to 330°, while Io moved from 70° to 110° phase. This is thus one of the class of Io-related storms associated with Io phase near 90° (see Figure 3c). But unlike the strictly-confined source regions observed at higher frequencies, this storm continued nearly uninterrupted for about 170° of CML, or nearly half a planetary rotation. It is of interest then to examine the polarization of the s-bursts throughout this interval to uncover possible systematic variations in polarization sense and so determine what segment of the Io flux tube (i.e. north or south) is beaming radiation toward the observer at a given time.

Except for a few s-bursts exhibiting weak LH polarization, all of the bursts observed between 1240 and 1350 SCET were RH polarized. The CML-Io

phase geometry during this time corresponded to that of an Io-B storm according to the definition that applies at higher frequencies. The observed s-burst polarization is also consistent with the dominant polarization (RH) of this source as measured at higher frequencies (see Carr et al. [1983]). Beyond this time, although the storm can no longer be termed "Io-B", the s-bursts continued to be RH polarized until about 1530. Between 1530 and 1550 the s-bursts were too weak and narrow banded for reliable sense determination, but beginning at 1550 and continuing until the end of the storm at 1730, the s-bursts were exclusively LH polarized. Thus the storm underwent a clear polarization reversal somewhere between 260° and 280° CML, being predominantly RH polarized below this longitude range and exclusively LH above it.

These observations are summarized in Figure 6 where we show, above the figure, the observed polarization sense as a function of CML in the form of a white bar denoting RH and black bars denoting LH-polarized emission. The gap from 260° - 280° CML corresponds to the time when only weak s-bursts were observed and no polarization information was available. This figure also illustrates what we consider to be a plausible explanation for the pronounced polarization reversal observed during the course of this storm. We define θ as the angle between the radius vector to the observer and Jupiter's magnetic field direction (from the O_4 magnetic field model) at the s-burst source. Two possible source locations have been assumed: one in the northern hemisphere and one in the southern hemisphere, each at the position on the Io flux tube (IFT) corresponding to the 10 MHz local electron gyrofrequency. The solid (dashed) curve shows how θ varies with CML for the north (south) IFT source. This is to be compared with the lightly shaded area of the figure which illustrates the inferred geometry of the emission. There is ample evidence from previous studies both experimental and theoretical that the Io-stimulated emission is beamed at an angle near 90° to the field line into a narrow cone of radiation (see, e.g., Goldstein and Goertz [1983]). In our analysis we have centered a 14°-wide radiation beam at θ = 90° because we find that this location best matches the observed start and stop times of the 12 July storm. It is then apparent from Figure 6 that for longitudes between 160° and 250°, only the north IFT source emission is observable since the observer is within the emission cone for that source but outside the south IFT emission cone. However, for longitudes between 250° and 330°, the observer is only within the

south IFT emission cone, and hence can only observe radiation from the southern hemisphere source. Note that for extraordinary mode radiation, these source locations correspond to RH and LH respectively. Comparison with Figure 5 shows that these predicted polarizations agree with the dominant polarization senses observed during the storm.

In conclusion, several features of the 12 July storm are consistent with this model. First, the reversal in polarization is predicted to occur at about 250° CML and is actually observed to take place somewhere between 260° and 280° CML. Second, near this crossover longitude the bursts should also appear weak since the observer is on the edge of the emission beam. Finally, the observed sense of polarization agrees with the expected polarization for extraordinary mode emission from the two source regions.

Two additional storms, comprised of a total of 28 s-bursts, have been examined to help verify this picture. The first, at 0930 on 4 March 1979 (130° CML, 89° ϕ_{Io}), was observed to be RH polarized. According to the beaming model shown in Figure 6, the observer was within the radiation cone of both the north and south IFT sources ($\theta \sim 88°$). Apparently only the north IFT source was active at the time of the observation. The second storm, at $\sim$ 2025 on 28 February 1979 (301° CML, 106° ϕ_{Io}), was LH polarized and according to our model only LH polarized emission should have been observed.

Summary

The emphasis in this study differs from most analyses of Voyager radio observations of Jovian decametric radiation performed to date because we have concentrated on the very short time-scale (< 100 ms) bursts rather than the longer time-scale ($\gtrsim$ 1 min) features that characterize most of Jupiter's emissions. The only previous discussion of Voyager measurements of s-bursts [Leblanc and Genova, 1981] was restricted to frequencies above 15 MHz, and our survey extends the analysis into the 5 to 15 MHz range where the Voyager instrument is especially sensitive for observations of decametric s-bursts. Measurements at such low frequencies are particularly difficult to obtain from the ground, and thus the only comparable measurements are those obtained by Ellis and co-workers [Ellis, 1982] from the University of Tasmania.

Our initial analysis of the Voyager s-burst data near 10 MHz has led to three principal conclusions:

1. The low frequency s-bursts can be found at essentially all values of CML, but they are strongly dependent on Io-phase with occurrence maxima centered at ϕIo = 90° and 230°. We agree with the conclusion drawn by Withham [1978] that this pattern suggests that the s-bursts are generated in a source in the Io flux tube, and we believe this is the most direct evidence yet for a component of Jupiter's decametric radiation that is uniquely associated with the instantaneous Io flux tube. Details of the distribution of s-bursts in the CML - ϕIo plane (e.g., the kink in the ϕIo = 90° band at CML = 150° and the gap in the ϕIo = 230° band at CML = 195° ± 45° in Figure 3c) need to be studied further to determine whether they can be explained quantitatively in terms off asymmetries in the magnetic field topology and wave propagation geometry near Jupiter.

2. Individual s-bursts often extend over a total frequency range of about 2 MHz, and they sometimes span a frequency range of at least 3 MHz. For an emission mechanism that involves radiation at the electron gyrofrequency by particles ascending a specific bundle of magnetic field lines, this frequency range corresponds to a linear dimension of 4000 to 6500 km along which the electron beam must maintain the degree of coherence necessary to generate an s-burst.

3. S-bursts usually exhibit a significant degree of circular polarization, but the polarization sense is not a simple, systematic function of CML or ϕIo. The polarization data suggest that s-bursts can be generated along either the northern hemisphere or southern hemisphere Io flux tube, but that their visibility for an observer at a specific location probably depends on the geometric properties of the burst radiation pattern. More work is needed, both in analysis of the Voyager data and in the collection of ground-based data, in order to understand and interpret the polarization properties of s-bursts.

Acknowledgments

We are pleased to thank B. Razzaghinijad and M. Schwee for their assistance in the processing and display of the Voyager dynamic spectra. We also acknowledge the helpful discussions with our colleagues M. Kaiser and Y. Leblanc. The remarkable versatility and capability of the Voyager Planetary Radio Astronomy receivers are largely due to the early design efforts of J. W. Warwick (Principal Investigator) and R. G. Peltzer.

References

Acuna, M. H. and N. F. Ness, Results from the GSFC fluxgate magnetometer on Pioneer 11, in Jupiter, ed. T. Gehrels, pp. 830-847, Univ. of Arizona Press, 1976.

Alexander, J. K., T. D. Carr, J. R. Thieman, J. J. Schauble and A. C. Riddle, Synoptic observations of Jupiter's radio emissions: Average statistical properties observed by Voyager, J. Geophys. Res., 86, 8529-8545, 1981.

Boischot, A., A. Lecacheux, M. L. Kaiser, M. D. Desch and J. K. Alexander, J. Geophys. Res., 86, 8213-8226, 1981.

Carr, T. D., M. D. Desch and J. K. Alexander, Phenomenology of magnetospheric radio emissions, in Physics of the Jovian Magnetosphere, ed. A. J. Dessler, pp. 226-284, Cambridge Univ. Press, 1983.

Desch, M. D., R. S. Flagg and J. May, Jovian S-burst observations at 32 MHz, Nature, 272, 38-40, 1978.

Ellis, G. R. A., An atlas of selected spectra of the Jupiter s-bursts, Univ. of Tasmania, Hobart, 1979.

Ellis, G. R. A., The source of the Jupiter S-bursts, Nature, 283, 48-50, 1980.

Ellis, G. R. A., Observations of the Jupiter S-bursts between 3.2 and 32 MHz, Aust. J. Phys., 35, 165-175, 1982.

Genova, F., M. G. Aubier and A. Lecacheux, Modulations in Jovian decametric spectra: Propagation effects in terrestrial ionosphere and Jovian environment, Astron. Astrophys., 104, 229-239, 1981.

Goldstein, M. L. and C. K. Goertz, Theories of radio emissions and plasma waves, in Physics of the Jovian Magnetosphere, ed. A. J. Dessler, pp. 317-352, Cambridge Univ. Press, 1983.

Lang, G. J. and R. G. Peltzer, Planetary radio astronomy receiver, IEEE Trans., AES13, 466, 1977.

Leblanc, Y. and F. Genova, The Jovian s-burst sources, J. Geophys. Res., 86, 8564-8568, 1980.

Leblanc, Y., F. Genova and J. de la Noe, The Jovian s-bursts. I. Occurrence with L-bursts and frequency limit, Astron. Astrophys., 86, 342-348, 1980.

Leblanc, Y. and M. Rubio, A narrow-band splitting at the jovian decametric cutoff frequency, Astron. Astrophys., 111, 284-294, 1982.

Riihimaa, J. J., Modulation lanes in the dynamic spectra of Jovian L bursts, Astron. Astrophys., 4, 180-188, 1970.

Riihimaa, J. J., S-bursts in Jupiter's decametric radio spectra, Astrophys. Space Sci., 51, 363-383, 1977.

Witham, P. S., Jupiter's S bursts and Io, Nature, 272, 40-41, 1978.

Figure Captions

Figure 1. A schematic view of how the Voyager Planetary Radio Astronomy receiver sampling scheme permits detection of s-bursts.

Figure 2. Frequency-time dynamic spectra of Jovian decametric emissions for three representative 1-hour intervals during which s-bursts were observed.

Figure 3. (a) The occurrence of s-burst storms observed at frequencies in the range 15-25 MHz plotted as a function of System III (1965) Central Meridian Longitude and Io phase. (b) Same as above but for s-bursts in the 5-15 MHz frequency range. (c) The relative probability of occurrence of s-bursts between 15 and 25 MHz (shaded histogram) and between 5 and 15 MHz (open histogram) plotted as a function of Io phase.

Figure 4. Histogram of the distribution of maximum frequency extent observed for s-burst storms centered near 10 MHz.

Figure 5. The polarization sense of the s-burst storms as a function of Central Meridian Longitude and Io phase. The legend at the top shows sense convention.

Figure 6. The angle θ between the local magnetic field direction in the O_4 model and the observer's direction is shown as a function of CML for the north (solid) and south (dashed) IFT. The shaded region illustrates the s-burst beam geometry inferred in this paper. The observed polarization sense for the 12 July storm is shown by the bars above the figure.

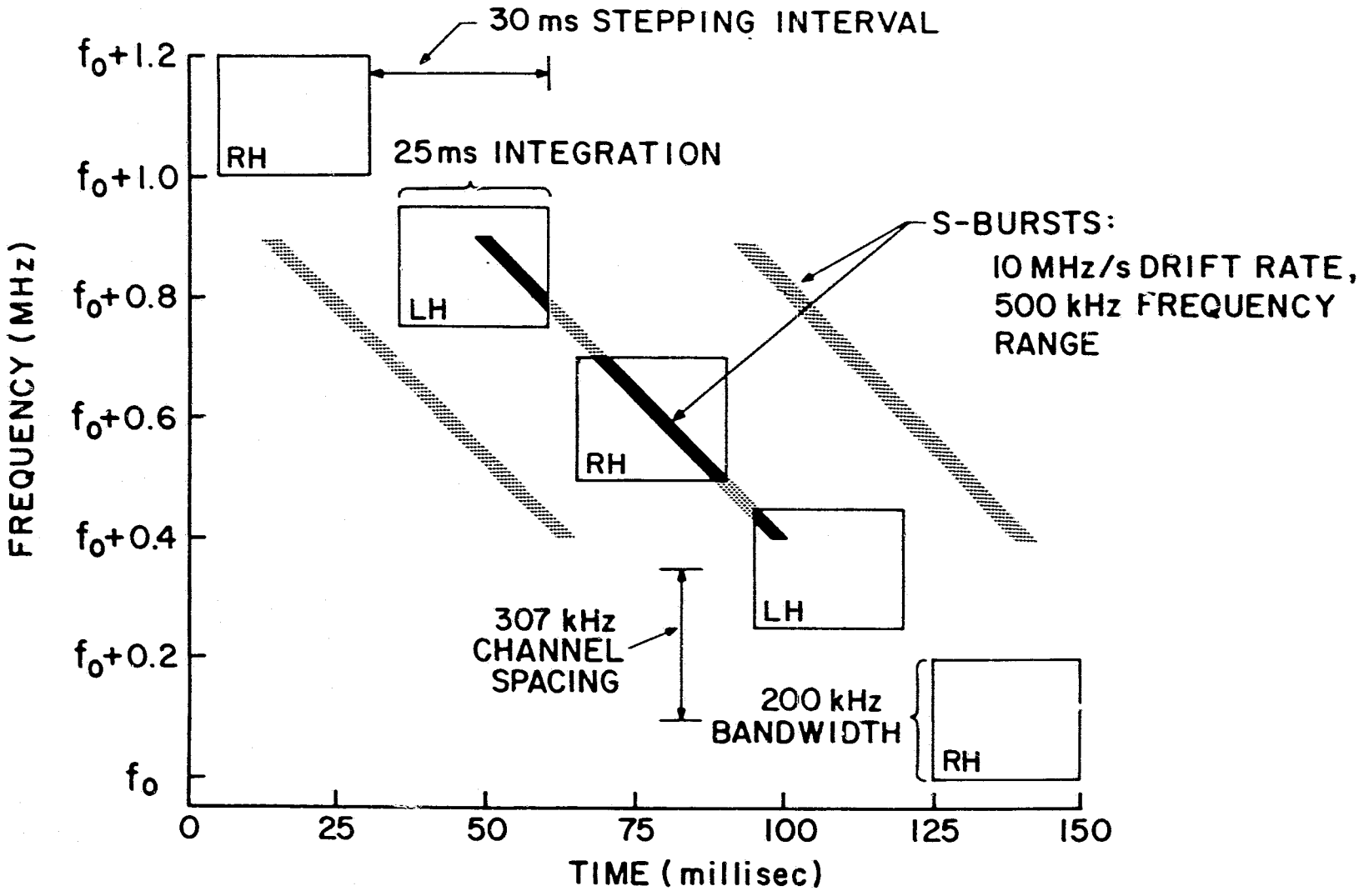

FIGURE 1

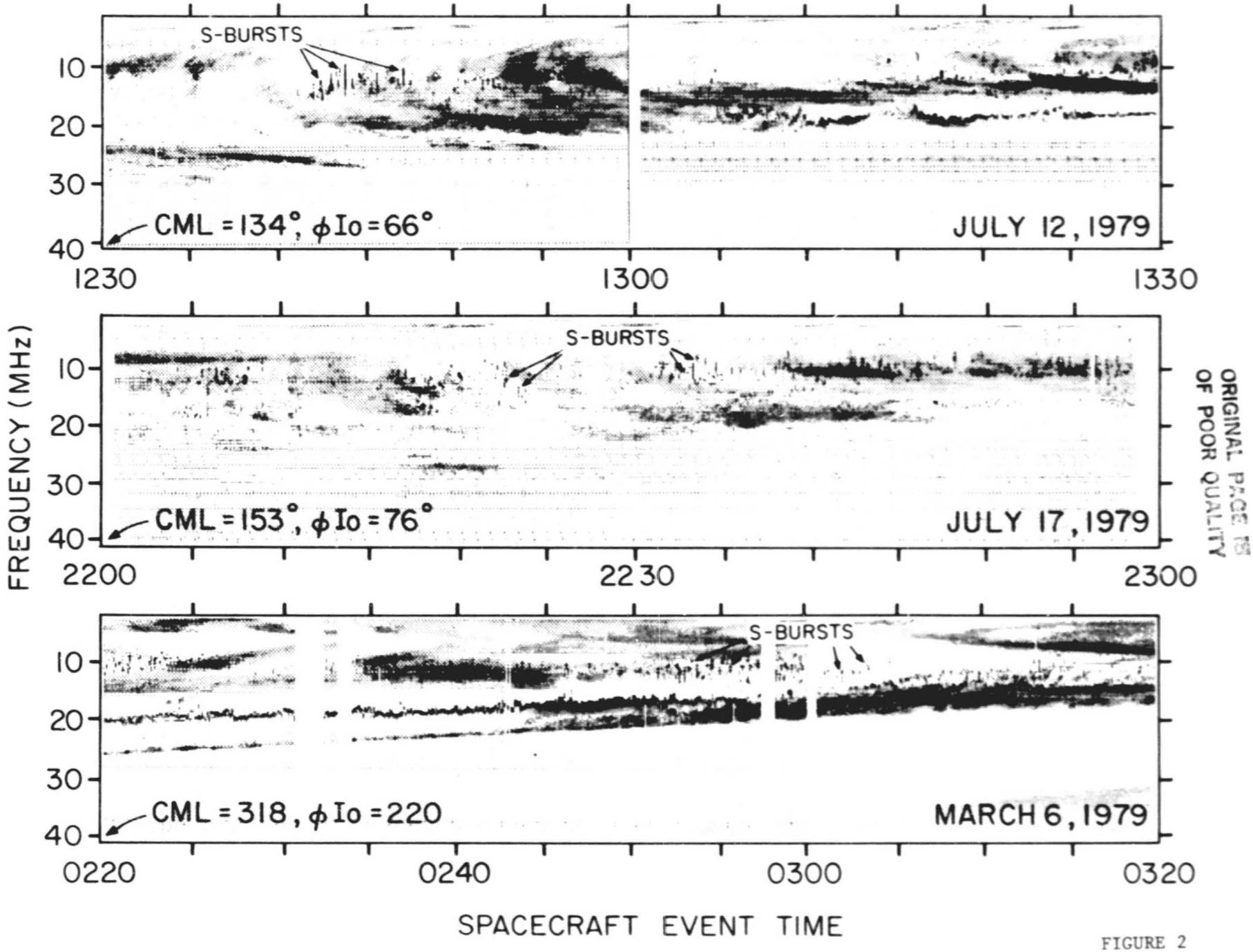

FIGURE 2

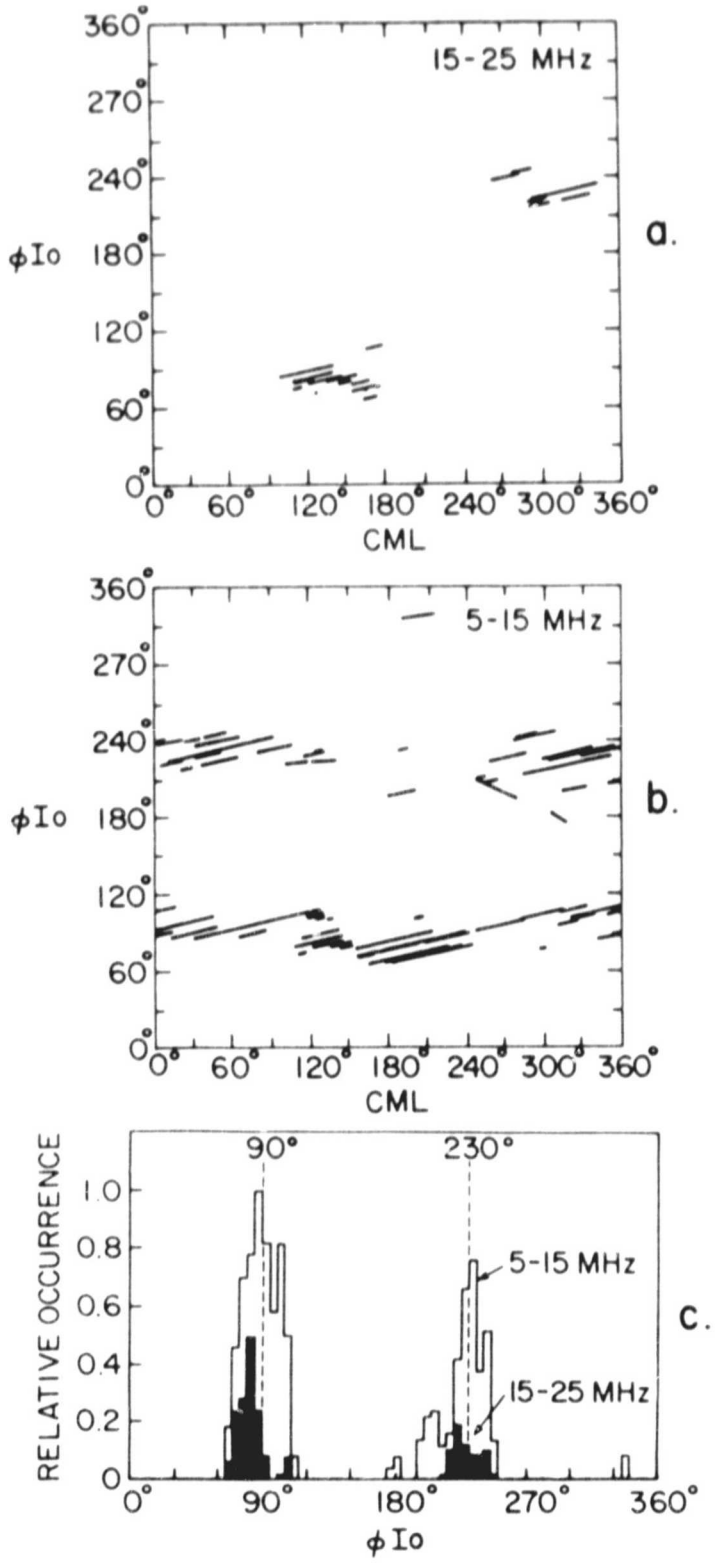

FIGURE 3

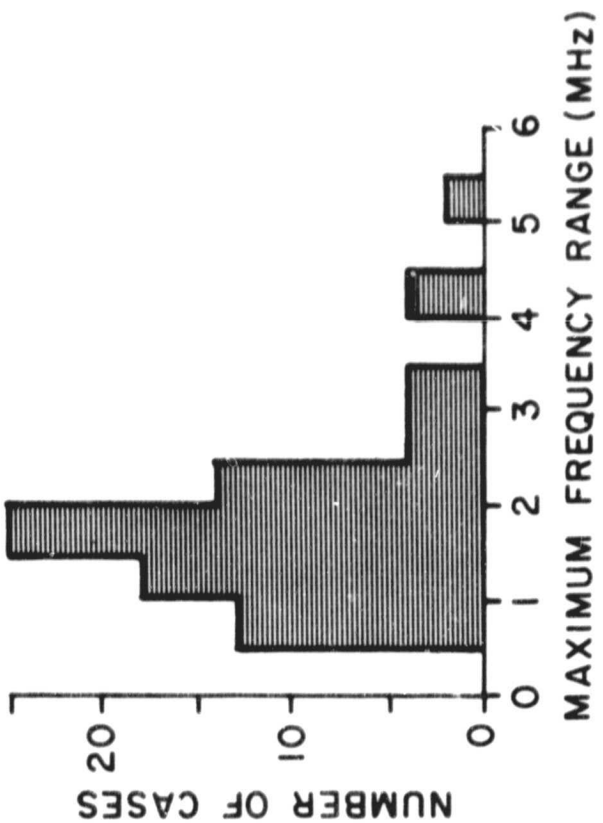

FIGURE 4

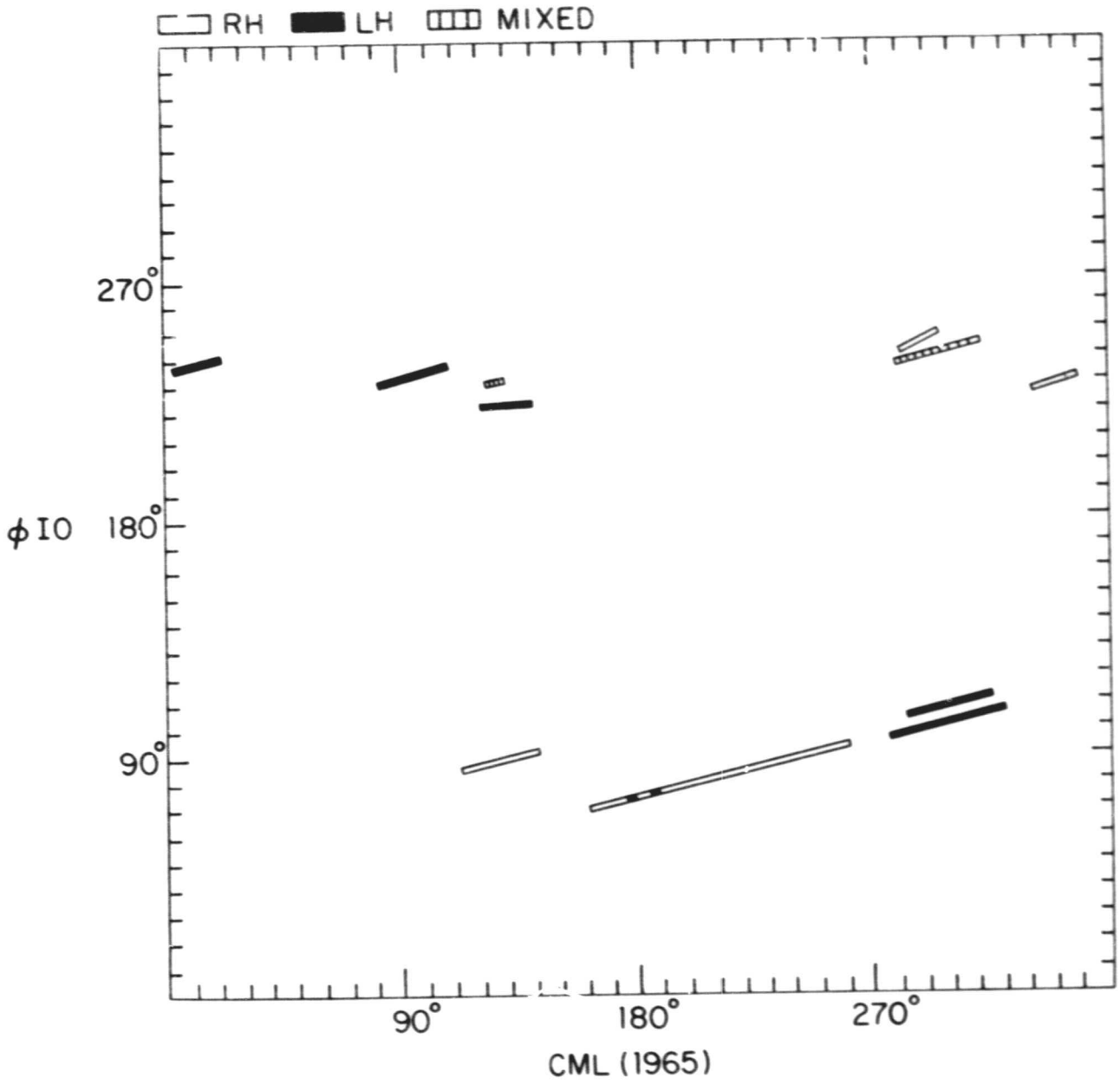

FIGURE 5

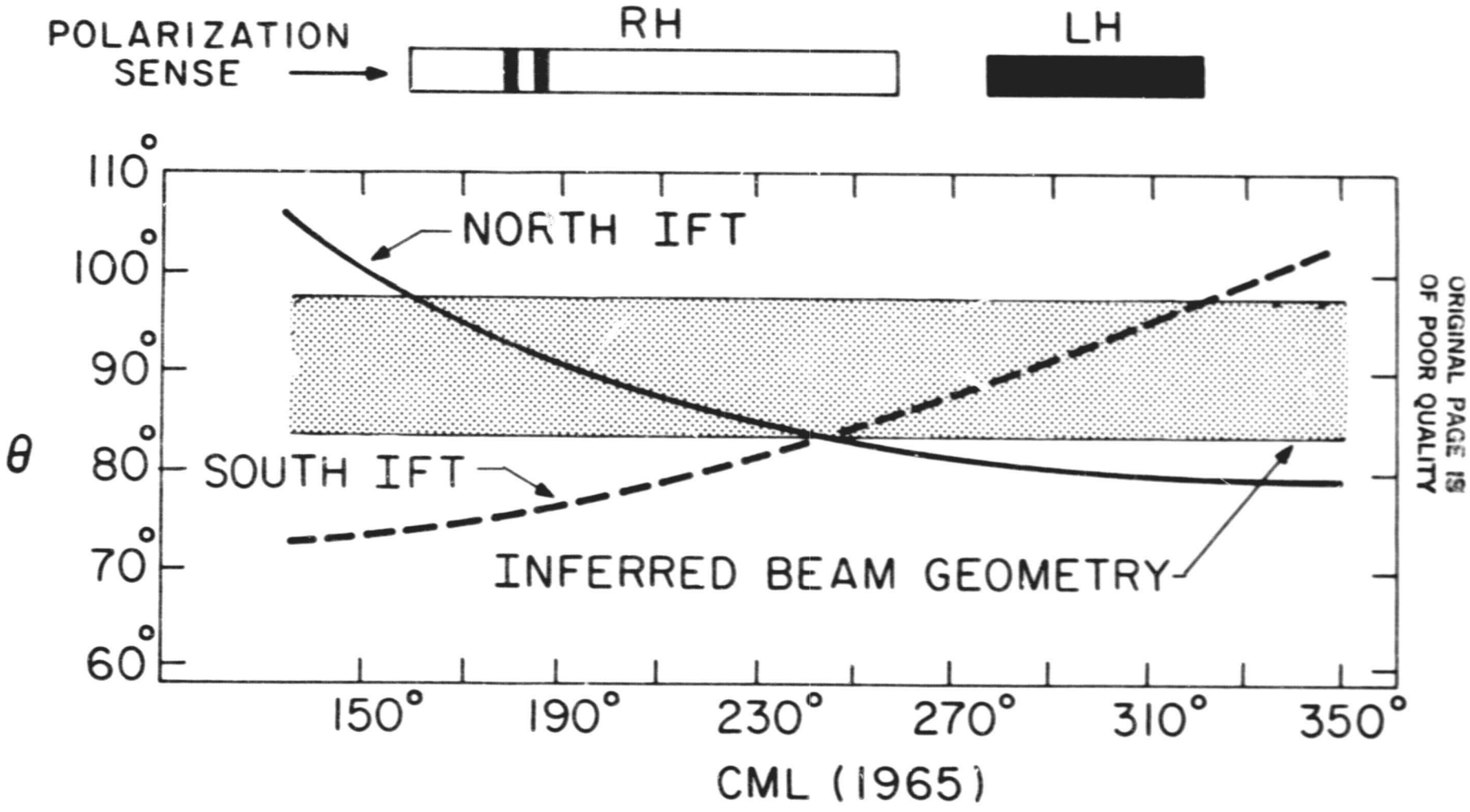
POLARIZATION SENSE
RH
LH
110°
100°
90°
80°
70°
60°
θ
NORTH IFT
SOUTH IFT
INFERRED BEAM GEOMETRY
150°
190°
230°
270°
310°
350°
CML (1965)
ORIGINAL PAGE IS OF POOR QUALITY

FIGURE 6